Molecular Dynamics Simulation of Benzenethiolate and Benzyl Mercaptide on Au(111)

Hun Huy Jung,† Young Do Won,‡ Seokmin Shin,† and Kwan Kim*,†

Department of Chemistry and Center for Molecular Catalysis, Seoul National University, Seoul 151-742, Korea, and Department of Chemistry, Han Yang University, Seoul 133-791, Korea

Received July 13, 1998. In Final Form: November 23, 1998

We report the results of theoretical studies on the self-assembled monolayers of benzenethiolate (BT) and benzyl mercaptide (BZM) on a Au(111) surface. A few relevant potential energy parameters were determined. We have performed annealing type molecular dynamics simulations where the minimized initial configurations are heated to 1000 K and then cooled to room temperature, assuming two types of unit cells: $\sqrt{3} \times \sqrt{3}R30°$ and 2×2. The results of the simulations showed that BZM formed a nearly perfect herringbone structure, while the apparent herringbone type structure of BT was somewhat disordered in the $\sqrt{3} \times \sqrt{3}R30°$ unit cell. For the 2×2 unit cell with larger area per molecule, both monolayers did not form well-ordered structures, but the BZM showed some local ordering with herringbone structure. In both cases, the molecules of BZM are found to be nearly vertical to the surface, while those of BT are tilted from the surface normal. All these theoretical results are consistent with recent experimental findings. The role of a flexible methylene unit near the sulfur headgroup in discriminating stable packing structures of the self-assembled monolayers is discussed.

Introduction

In the past decade, self-assembled monolayers (SAMs) of organic molecules on metal surfaces, in particular those of thiol molecules on Au(111), have attracted much attention, not only from the scientific point of view of better understanding phenomena such as heterogeneous catalysis, adhesion, lubrication, and corrosion, but also from their practical applicability.[1−3] Recent interest has focused on the application prospects of SAMs for efficient electronic and optical devices, chemical sensors, artificial membranes, and electron-transfer barriers.

Alkanethiol molecules on gold surfaces have been the most widely studied SAM system.[4−9] From the LEED studies, Dubois et al. observed well-ordered monolayers when alkanethiol molecules were adsorbed on Au(111) in a gas phase.[6] Longer alkanethiol molecules were found to assume a $m\sqrt{3} \times \sqrt{3}R\ 30°$ ($m = 4-6$) structure while small molecules such as methanethiol and ethanethiol formed a $\sqrt{3} \times \sqrt{3}R30°$ structure. Interestingly, when longer alkanethiols were self-assembled on Au(111) in a solution phase, STM and AFM observations showed the thiol monolayers to have a $\sqrt{3} \times \sqrt{3}R30°$ structure.

Compared with alkanethiols, relatively few experimental studies have been done on the SAMs of aromatic thiols on Au(111), particularly when formed in the solution phase.[10−12] Recently, Tao et al. reported that the structural order of self-assembled monolayers of benzenethiolate and biphenylthiolate on Au(111) is very poor while the benzyl mercaptide and 4-biphenylmethanethiolate monolayers are well-ordered with a commensurate $\sqrt{3} \times \sqrt{3}R30°$ structure.[11] When an alkoxy chain was substituted at the para position of the benzene ring moiety, similar structures were observed in the STM images. The presence of a methylene unit between the sulfur headgroup and benzene ring was suggested to play an important role in the ordering of such self-assembled monolayers.

In the past decade, molecular dynamics (MD) simulations have emerged as a useful means, complementary to various experimental techniques, to provide the structural and dynamical properties of SAMs of organic molecules on metal surfaces.[13−24] For instance, Klein and his colleagues have demonstrated their utility by identifying and classifying structural phases of an $Au/S(CH_2)_{15}CH_3$ monolayer, at least qualitatively in consonance with the

* To whom all correspondence should be addressed. Tel: 82-2-880-6651. Fax: 82-2-874-3704 or 82-2-889-1568. E-mail: kwankim@plaza.snu.ac.kr.

† Seoul National University.

‡ Han Yang University.

(1) Ulman, A. *An Introduction to Ultrathin Organic Films*; Academic Press: Boston, MA, 1991.
(2) Ulman, A. *Chem. Rev.* **1996**, *96*, 1533.
(3) Dubois, L. H.; Nuzzo, R. G. *Annu. Rev. Phys. Chem.* **1992**, *43*, 437.
(4) Porter, M. D.; Bright, T. B.; Allara, D. L.; Chidsey, C. E. D. *J. Am. Chem. Soc.* **1987**, *109*, 3559.
(5) Nuzzo, R. G.; Dubois, L. H.; Allara, D. L. *J. Am. Chem. Soc.* **1990**, *112*, 558.
(6) Dubois, L. H.; Zegarski, B. R.; Nuzzo, R. G. *J. Am. Chem. Soc.* **1990**, *112*, 570.
(7) Walczak, M. M.; Chung, C.; Stole, S. M.; Widrig, C. A.; Porter, M. D. *J. Am. Chem. Soc.* **1991**, *113*, 2370.
(8) Labinis, P. E.; Whitesides, G. M.; Allara, D. L.; Tao, Y.-T.; Parikh, A. N.; Nuzzo, R. G. *J. Am. Chem. Soc.* **1991**, *113*, 7152.
(9) Alves, C. A.; Smith, E. L.; Porter, M. D. *J. Am. Chem. Soc.* **1992**, *114*, 1222.
(10) Sabatini, E.; Cohen-Boulakia, J.; Bruening, M.; Rubinstein, I. *Langmuir* **1993**, *9*, 2974.
(11) Tao, Y.-T.; Wu, C.-C.; Eu, J.-Y.; Lin, W.-L. *Langmuir* **1997**, *13*, 4018.
(12) Dhirani, A.-A.; Zehner, R. W.; Hsung, R. P.; Guyot-Sionnest, P.; Sita, L. R. *J. Am. Chem. Soc.* **1996**, *118*, 3319.
(13) Hautman, J.; Klein, M. L. *J. Chem. Phys.* **1989**, *91*, 4994.
(14) Hautman, J.; Klein, M. L. *J. Chem. Phys.* **1990**, *93*, 7483.
(15) Bareman, J. P.; Klein, M. L. *J. Phys. Chem.* **1990**, *94*, 5202.
(16) Hautman, J.; Bareman, J. P.; Mar, W.; Klein, M. L. *J. Chem. Soc., Faraday Trans.* **1991**, *87*, 2031.
(17) Mar, W.; Klein, M. L. *Langmuir* **1994**, *10*, 188.
(18) Taut, C.; Pertsin, A. J.; Grunze, M. *Langmuir* **1996**, *12*, 3481.
(19) Zhang, Z.; Beck, T. L.; Young, J. T.; Boerio, F. J. *Langmuir* **1996**, *12*, 1227.
(20) Mahaffy, R.; Bhatia, R.; Garrison, B. J. *J. Phys. Chem. B* **1997**, *101*, 771.
(21) Morgner, H. *Langmuir* **1997**, *13*, 3990.
(22) Bhatia, R.; Garrison, B. J. *Langmuir* **1997**, *13*, 765.
(23) Bhatia, R.; Garrison, B. J. *Langmuir* **1997**, *13*, 4038.
(24) Li, T.-W.; Chao, I.; Tao, Y.-T. *J. Phys. Chem. B* **1998**, *102*, 2935.

10.1021/la9808667 CCC: $18.00
Published on Web 01/26/1999

experimental observation.[13−17] MD simulations suggested that the stable crystalline structure of alkanethiol monolayers at low temperature is the herringbone (two-chain unit cell) structure, and at higher temperatures, the chains begin to rotate to give a four-site distribution. Eventually the system undergoes a transition to a rotator phase where the chains rotate almost freely and gauche defects form throughout the film. Zhang et al. have reported the molecular dynamics simulations of organic thiol monolayers such as (4-mercaptophenyl)phthalimide (4-MPP) on gold surface.[19] The overall appearance of the 4-MPP system was found to be a dense but disordered monolayer. The results from the molecular dynamics simulations for SAMs of 4′-alkoxybiphenyl-4-thiols on the Au(111) surface by Li et al. suggested that the flexibility of the headgroup influences the variety of possible packing structures.[24]

In conjunction with the above implications, we have performed molecular mechanics calculations and molecular dynamics simulations for benzenethiolate and benzyl mercaptide monolayers self-assembled on a Au(111) surface. The main motivation is to provide a better understanding of the close-packed structures of these molecules on gold; the intent is to know the role of the flexible methylene group in determining the final structures of full-covered SAMs of these molecules on Au(111).

Model

Since organic thiols are known to chemisorb on gold as thiolates after the deprotonation of the S−H bonds, we assume the adsorbates to reside on the Au(111) surface exclusively as benzenethiolate (BT) or benzyl mercaptide (BZM). In Figure 1 are depicted the definitions of geometry of BT and BZM on gold in terms of three angles. The tilt angle, θ, is defined as the angle between the surface normal and the molecular axis. The twist angle, ψ, of a benzene ring is obtained from the angle made by two vectors, one being defined as a cross product between vectors of the molecular axis and the surface normal and the other being the one perpendicular to the molecular plane. The azimuthal angle, ϕ, is defined as the angle between the *y*-axis of a unit cell and the projection of the molecular axis on the surface.

Regarding the binding site of the sulfur headgroup, it has generally been accepted that the sulfur atoms are located at the 3-fold hollow sites of the Au(111) surface. According to the quantum mechanical calculation by Sellers et al.,[25] two types of bonding schemes, sp and sp^3 type, seemed possible for sulfur when HS^- and CH_3S^- interact with the gold atoms of Au(111); in either case, the sulfur atom appeared, however, to be located at the 3-fold hollow site. On these grounds, the sulfur atom of BT or BZM molecule was assumed to interact exclusively with three gold atoms at a 3-fold hollow site on the surface layer.

Recalling the literature data, the smallest unit cell for a full-covered thiolate monolayer on Au(111) should be a $\sqrt{3} \times \sqrt{3}R30°$ structure, corresponding to 21.3 Å^2/molecule. The next and third possible ones are conjectured to be the 2×2 and $\sqrt{7} \times \sqrt{7}R40.9°$ structures, respectively. Considering that the inverse bonding densities of the latter two unit cells are 28.8 and 50.4 Å^2/molecule, respectively, any thiolate monolayer whose inverse bonding density is between those two values may not be described in terms of a commensurate unit cell. The electrochemical measurement by Tao et al.[11] showed that the amounts of benzyl mercaptide derivatives on Au(111) at a full-coverage limit

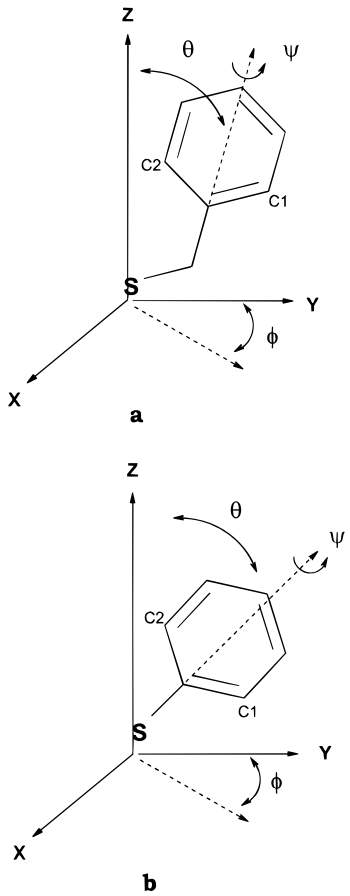

Figure 1. Angles describing the orientations of (a) benzyl mercaptide (BZM) and (b) benzenethiolate (BT) molecules on a surface. Detailed definitions for the tilt angle (θ), the twist angle (ψ), and the azimuthal angle(ϕ) are given in the text.

was quite similar, irrespective of the substituent group on the aromatic ring, assuming 21.3 Å^2/molecule. Since the latter value matches well with that of the $\sqrt{3} \times \sqrt{3}R30°$ structure, we have assumed that the BZM molecules arrange on Au(111) exclusively with lattices commensurate with $\sqrt{3} \times \sqrt{3}\,R30°$ unit cells with the average nearest neighbor distance of 5.00 Å. For BT molecules, the close-packed arrangement on Au(111) is known incommensurate with any small-sized unit cells. For instance, according to Tao et al., the packing density of BT derivatives depended very much on the substituent group, ranging from 37.8 Å^2/molecule for BT itself to 25.2 Å^2/molecule for hexadecyloxy-substituted BT. Nonetheless, for comparative purposes with BZM, we assumed the $\sqrt{3} \times \sqrt{3}R30°$ structure to hold even for BT on Au(111). In addition, since the surface area of a 2×2 unit cell is somewhat close to the measured inverse bonding density of BT, we have adopted the 2×2 structure, in which the average nearest neighbor distance is 5.77 Å, in the MD simulations of BZM as well as BT at 300 K.

Simulation Method

All the MD simulations have been performed by using the CHARMM program;[26] either the academic version of the CHARMM-25 package on a HP/730 workstation or the commercial version of the CHARMM-24 package on an IBM SP2 RS/6000 platform. Under the CHARMM force field, the interaction energy consists of internal, i.e., intramolecular, and external, i.e., intermolecular, potential energies. The bond stretching, angle

(25) Sellers, H.; Ulman, A.; Shnidman, Y.; Eilers, J. E. *J. Am. Chem. Soc.* **1993**, *115*, 9389.

(26) Brooks, B. R.; Bruccoleri, R. E.; Olafson, B. D.; Statos, D. J.; Swaminathan, S.; Kaplus, M. *J. Comput. Chem.* **1983**, *4*, 187.

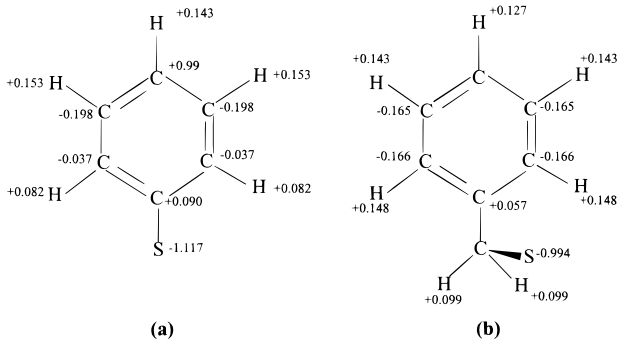

Figure 2. Point charges of (a) BT and (b) BZM used in MD simulations (units are e's). See the text for details.

bending, and dihedral angle torsion terms are included to represent the internal potential energy, along with the nonbonded van der Waals (vdW) and electrostatic interaction terms. The external potential energy contains also the vdW and the electrostatic interaction terms. In this work, the internal parameters that are related with the Au−S and S−C bond stretching, the Au−S−C angle bending, and the Au−S−C−C and S−C−C−C dihedral angle torsion motions as well as the external parameters that are related with the electrostatic interaction terms are determined as described below. Otherwise, all the potential energy parameters are taken exclusively from those implemented in the CHARMM program.[27]

Regarding the electrostatic interaction terms, we have obtained the optimized geometries of neutral molecules, i.e., benzenethiol and benzyl mercaptan, along with their atomic charges by using the Gaussian 94 program at RHF/6-31G** level. For a better fit to the electrostatic potential, the so-called Merz−Singh−Kollman scheme was employed in the population analysis. We assumed the hydrogen atom bonded to sulfur to be removed as a proton (+1 charged); some extra negative charge was thus adversely added to the sulfur atom. To take into account the molecular symmetries, the electronic charges were optimized further using an AMBER force field by referring to the method of Bayly et al.[28,29] The resulting charges are displayed in Figure 2.

For the internal interaction terms, the dihedral angle torsion potential was assumed to take the following form as included in the CHARMM program:

$$V_\varphi = k_\varphi[1 + \cos(n\varphi - \delta)] \qquad (1)$$

Here k_φ represents the dihedral force constant, n the periodicity, and δ the phase angle. To obtain the k_φ and δ values for the $S-C_{methylene}-C_{ring}-C_{ring}$ bonds of BZM, we have calculated the energy of benzyl mercaptan as a function of the corresponding dihedral angle (except for the dihedral angle, no constraint was imposed in the quantum mechanical geometry optimization routine at the RHF/6-31G** level). On the basis of eq 1, the relative energy was drawn as a function of dihedral angle (see Figure 3), and the best fitted parameters were determined to be 0.22 kcal/mol for k_φ and −19° for δ ($n = 2$ for BZM). To obtain the k_φ and δ values for the Au−S−C−C bonds of BT and BZM, we have attempted a similar quantum mechanical calculation. However, upon the incorporation of one gold atom, the geometry optimization could not be performed properly. Accordingly, we have assumed the dihedral parameters of the Au−S−C−C bonds to be similar to those of the C−C−C−C bonds implemented in the CHARMM program (considering the 2-fold rotational symmetry of benzene ring, the periodicity was also taken to be 2).

The Au−S and S−C bond lengths and the Au−S−C bond angle were allowed to vary with harmonic potentials, i.e., $2V_r = k_r(r - r_0)^2$, and $2V_\theta = k_\theta(\theta - \theta_0)^2$ in which k's are appropriate force constants and r_0 and θ_0 represent, respectively, the bond length

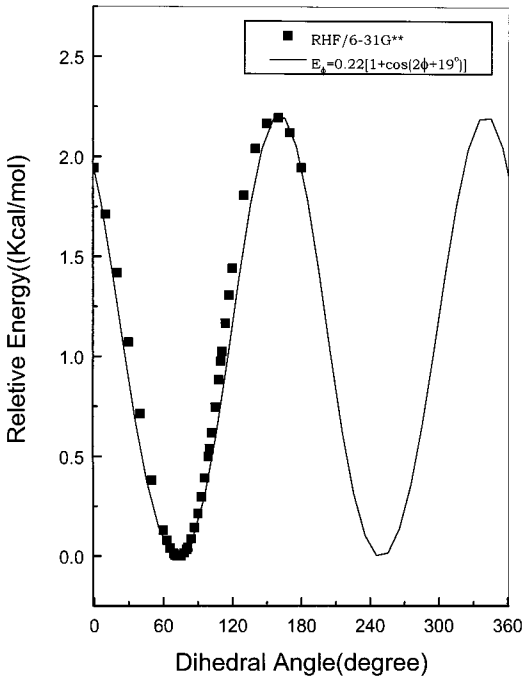

Figure 3. Dihedral angle potential energy for the $S-C_{methylene}-C_{ring}-C_{ring}$ bond of BZM. The results of ab initio calculations at the RHF/6-31G** level (■) are compared with the fitted curve to eq 1 in the text with parameters given in Table 1 (solid line).

and the bond angle in equilibrium states. To determine those parameters, we first considered one BT molecule residing at the 3-fold hollow site of the Au(111) surface (see below for the modeling of the gold surface), and performed the molecular mechanics calculation using the CHARMM program. We attempted to obtain the energy-minimized configuration on the gold surface. In this calculation, the point charges and the dihedral angle torsion potential parameters described above were used. We allowed the parameters related with the Au−S and S−C stretching and the Au−S−C bending potentials to vary around certain predetermined values; with reference to the literature data,[13,14,16] the parameters were varied in the ranges of $198.0 \pm a \times 80$ kcal/(mol·Å^2) ($a \le 2$) for $k_{r(Au-S)}$, $2.531 \pm b \times 0.5$ Å ($b \le 2$) for $r_{0(Au-S)}$, $205.0 \pm c \times 80$ kcal/(mol·Å^2) ($c \le 2$) for $k_{r(S-C)}$, $1.836 \pm d \times 0.5$ Å ($d \le 2$) for $r_{0(S-C)}$, $100.0 \pm e \times 20$ kcal/(mol·rad^2) ($e \le 4$) for $k_{\theta(Au-S-C)}$, and $120.0 \pm f \times 5$ deg ($f \le 3$) for θ_0. All other potential parameters were taken from the CHARMM program as default. We have selected the best values for the six parameters such that we would obtain the configuration of one BT molecule satisfying the following conditions: (i) The benzene ring should not be distorted. (ii) The S−C bond should lie on the benzene ring surface. (iii) The twist angle of the benzene ring should be 90° (or 270°) (see Figure 1). (iv) The benzene ring should be tilted by 10−30° with respect to the surface normal. (Condition iii is made to select physically reasonable configurations on the basis of the molecular symmetry of a single BT on a flat metal surface. Condition iv is made to allow that even the BT molecules could assemble into ordered herringbone structures.) It has to be noted that the adsorbate geometry is not greatly dependent on the above six parameters. The adsorbate structure was far more sensitive to the values of the nonbonded interaction (vdW and point charge) and the dihedral angle torsion parameters. The best optimized values are listed in Table 1.

To model the Au(111) surface, gold atoms were arranged hexagonally into two layers, assuming the nearest neighbor distance to be 2.88 Å. The positions of the gold atoms were fixed during all simulation; no explicit substrate relaxation was allowed. (Since the surface atoms were not allowed to move, two layers were sufficient for the anchoring of the sulfur headgroup to Au; additional layers barely affected the final results.) The charges of the gold atoms were set all to be zero. The sulfur headgroups were bound to three gold atoms at a 3-fold hollow site; since the harmonic force field was employed, the barrier between adjacent adsorption site should be enormous. We

(27) Momany, F. A.; Klimkowski, V. J.; Schafer, L. *J. Comput. Chem.* **1990**, *11*, 654.
(28) Bayly, C. I.; Cieplak, P.; Cornell, W. D.; Kollman, P. A. *J. Phys. Chem.* **1993**, *97*, 10269.
(29) Cornell, W. D.; Cieplak, P.; Bayly, C. I.; Kollman, P. A. *J. Am. Chem. Soc.* **1993**, *115*, 9620.

Table 1. Parameters for the Surface Interactions

(a) Bond Stretching: $E_{bond} = k_b(r - r_0)^2$

bond	r_0 (Å)	k_b (kcal/(mol· Å^2))
Au−S	2.531	198.0
S−C	1.836	205.0

(b) Angle Bending: $E_{angle} = k_\theta(\theta - \theta_0)^2$

angle	θ_0 (deg)	k_θ (kcal/(mol·rad^2))
Au−S−C	109.0	46.3468

(c) Dihedral Potential: $E_{dih} = k_\phi[1 + \cos(2\phi - \delta)]$

angle	δ (deg)	k_ϕ (kcal/mol)
Au−S−C−C	180.0	0.31
S−C−C−C (BZM)	−19.0	0.22

arranged 64 or 48 thiol molecules on the gold surface such as to encompass the $\sqrt{3} \times \sqrt{3}R30°$ and 2 × 2 unit cells, respectively. The overall shape of the system was rectangular, and a periodic boundary condition was imposed to reduce the edge effect. The benzene ring moieties were initially oriented randomly, and then any bad contacts were eliminated in a subsequent energy minimization. The minimization process was performed by the conjugate gradient and the adopted basis set Newton−Rapson methods. Thereafter, to circumvent the local minima problems, the temperature of the system was raised to 1000 K by performing MD simulation at a temperature increment of 5 K per 100 steps by velocity scaling. After being equilibrated at 1000 K for a sufficient period of time (about 100 ps), the system was slowly cooled to 300 K and equilibrated for another 100 ps. In all dynamics calculations, the time step was 1 fs and the dynamics productions were sampled at the intervals of 10 ps for about 100 ps. The cutoff distance related to the intermolecular interaction was 13 Å.

Results

Structures of BT and BZM on $\sqrt{3} \times \sqrt{3}R30°$ Unit Cells. In the initial configurations, the benzenethiolate (BT) and benzyl mercaptide (BZM) in both unit cells were configured such that their benzene rings were randomly oriented. In addition, the methylene units were all made to be parallel for the BZM SAMs. The minimized geometries of both monolayers were then ill-defined, however, implying that the structures of the SAMs might be trapped in local minima. For solving the problem of restricted initial geometry, at least partially, we heated the systems to a high enough temperature (e.g. 1000 K) and equilibrated them sufficiently at that temperature for 100 ps. Similar method has been used by Zhang et al. in the simulations for (4-mercaptophenyl)phthalimide (4-MPP) SAMs on various unit cells.[19] The equilibration time was found to be reasonable, because simulations over longer periods of equilibration gave similar results.

The initially randomized structures of both thiolates on the $\sqrt{3} \times \sqrt{3}R30°$ unit cell were becoming ordered in the form of herringbone structure during the equilibration at 1000 K, as monitored by the animations. After being cooled to 300 K and equilibrated for 100 ps, the BZM molecules, as can be seen in Figure 4a, formed a herringbone structure. Shown in Figure 4b, the structure of BT was also found to be herringbone-type, but it is not as well-defined as in the case of BZM. The benzene rings were nearly vertical to surface in BZM, but they were tilted in BT. The average tilt angle of BZM was found to be 9° ± 4°, and that of BT, 25° ± 6° (Figure 5). The molecules of BT were collectively tilted with rather narrow azimuthal angle distribution, as can be seen in Figure 6a. The four broad peaks of twist angle distribution of BT in Figure 6b indicated that the system was not represented by a single herringbone structure. It has also to be mentioned that when starting with initial configurations

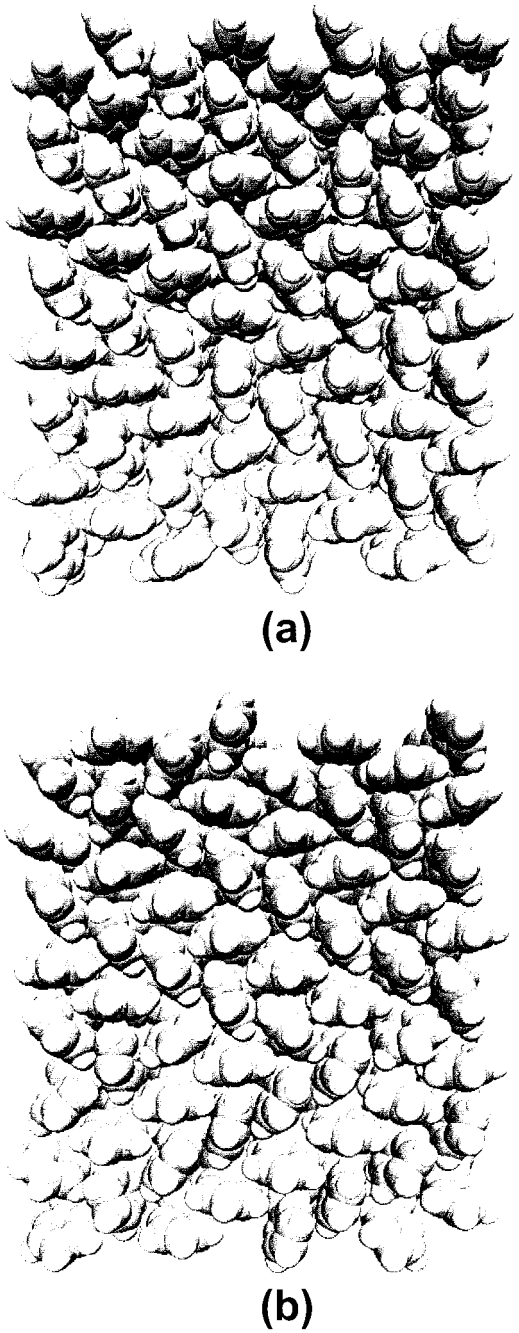

Figure 4. Snapshots of the configurations of (a) BZM and (b) BT on $\sqrt{3} \times \sqrt{3}R30°$ unit cells from the molecular dynamics simulations at 300 K.

where the orientations of the methylene units were randomly distributed, ordered herringbone structures were not obtained for the BZM monolayers.

Structures of BT and BZM on 2 × 2 Unit Cells. The surface structures of BZM and BT in 2 × 2 unit cells are shown in Figure 7a,b, respectively. The structures in the 2 × 2 unit cell were apparently different from those in $\sqrt{3} \times \sqrt{3}R30°$ unit cells. Well-defined herringbone structures were not found in both monolayers in 2 × 2 unit cells. Nonetheless, the BZM monolayer seemed to exhibit a formation of partially localized herringbone-type structure while the structure of BT was disordered. As can be seen in Figure 8a, the average tilt angle of BZM in a 2 × 2 unit cell was 14°(±8°), being not so much different from that in a $\sqrt{3} \times \sqrt{3}R30°$ unit cell. In contrast, the structure of BT in a 2 × 2 unit cell, shown in Figure 8b, exhibits the

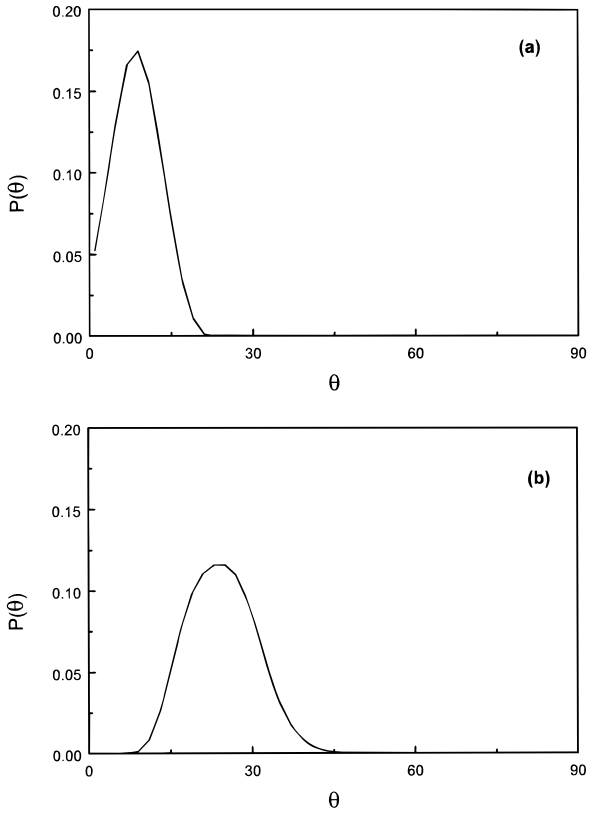

Figure 5. Distributions of tilt angle (θ) for (a) BZM and (b) BT on $\sqrt{3} \times \sqrt{3}R30°$ unit cells from the molecular dynamics simulations at 300 K.

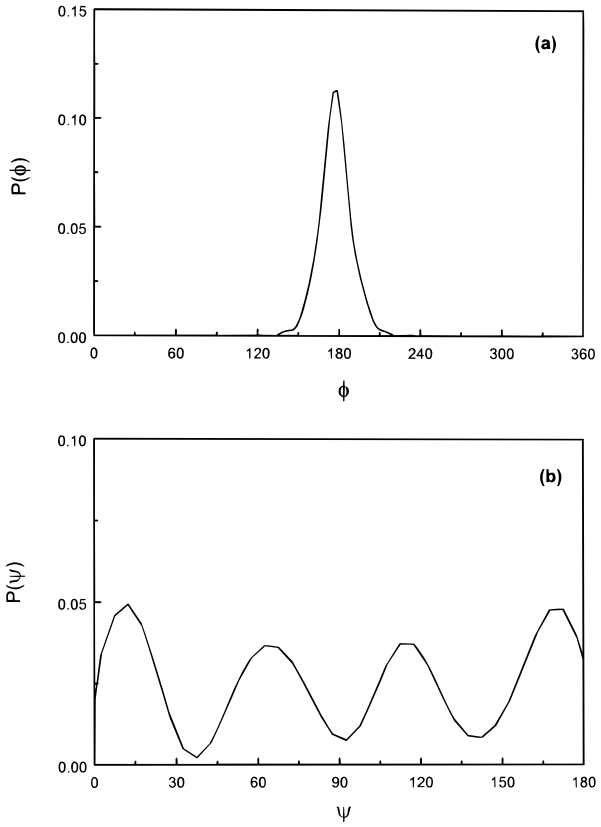

Figure 6. Distributions of (a) the azimuthal angle (ϕ) and (b) the twist angle (ψ) for BT on the $\sqrt{3} \times \sqrt{3}R30°$ unit cell from the molecular dynamics simulations at 300 K.

tilt angle distribution with the average of 42°(±8°), which is much larger than that in a $\sqrt{3} \times \sqrt{3}R30°$ unit cell. Large tilt angles of BT molecules resulted in clustering into locally dense region, as found in the simulations of 4-MPP by Zhang et al.[19] As can be seen in Figure 9a, the azimuthal angle distribution appears random for BZM, reflecting the very small tilt angles of BZM molecules. In contrast, the tilting directions of the molecules have rather narrow range in BT. The random distributions of the twist angles for the two monolayers, shown in Figure 10, indicate that there are no well-defined herringbone structures throughout the entire 2 × 2 unit cells; the orientations of the benzene rings are fluctuating during the simulations.

Discussion

It is impossible to simulate the whole process of self-assembly from the submonolayer in the initial stage to the full-covered monolayer. Instead we have performed simulations on two types of unit cells: $\sqrt{3} \times \sqrt{3}R30°$ and 2 × 2. The $\sqrt{3} \times \sqrt{3}R30°$ unit cell with the area of 21.6 Å^2/molecule would correspond to the close-packed, i.e., full-covered, monolayers for both BZM and BT. The results of the simulations showed that BZM formed a nearly perfect herringbone structure, while the apparent herringbone type structure of BT was not so well-defined. The important difference is that the molecules of BZM are vertical to the surface and those of BT are tilted from the surface normal. In fact, the difference in the molecular shapes of BT and BZM will affect the packing pattern of SAMs. Two bonding types (sp^3 and sp) of the sulfur atom may result in quite different orientations for the BT molecule (see Figure 11a); Sellers et al.[25] showed that both bonding types should be accessible at room temperature. Our potential parameters are, however, close to sp^3 bonding type (Table 1), which causes a considerable

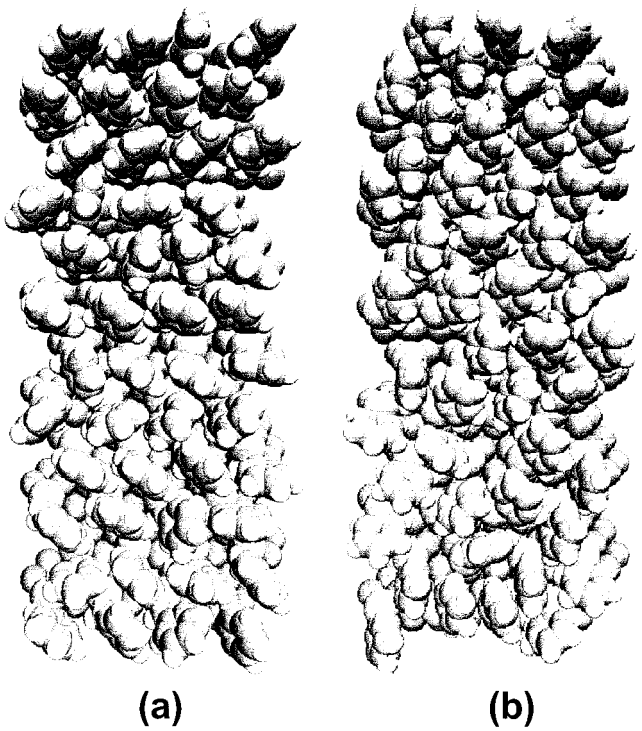

Figure 7. Snapshots of the configurations of (a) BZM and (b) BT on 2 × 2 unit cells from the molecular dynamics simulations at 300 K.

strain for the BT molecule to have vertical configuration at high densities. In contrast, BZM molecules can assume a rodlike structure (anti-form as shown in Figure 11b) due to the presence of the flexible CH_2 unit, which will

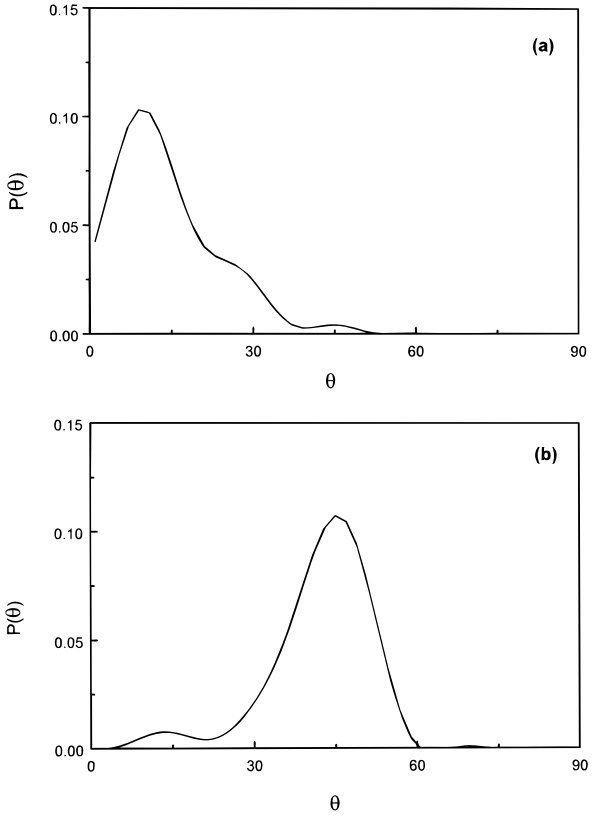

Figure 8. Distributions of the tilt angle (θ) for (a) BZM and (b) BT on 2 × 2 unit cells from the molecular dynamics simulations at 300 K.

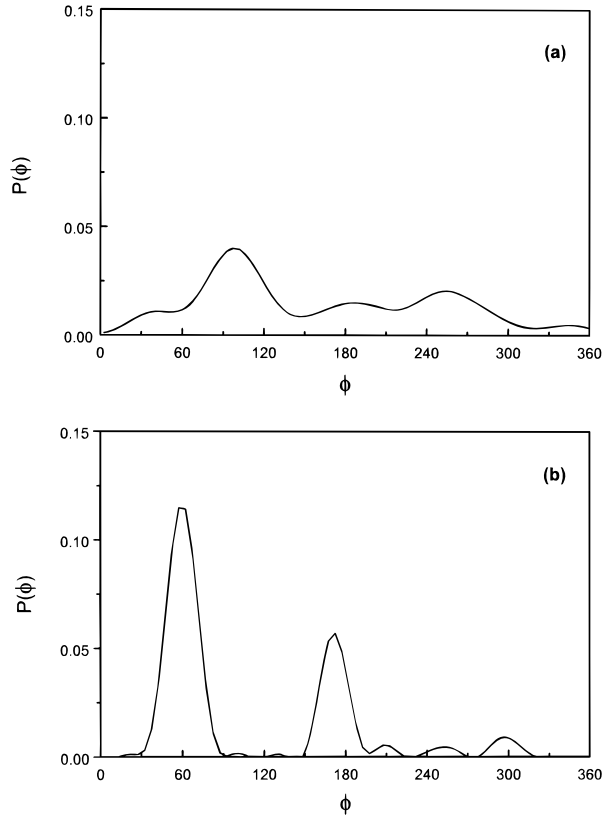

Figure 9. Distributions of the azimuthal angle (ϕ) for (a) BZM and (b) BT on 2 × 2 unit cells from the molecular dynamics simulations at 300 K.

allow them to have vertical configurations. It can be argued that having the molecules normal to the surface is advantageous to form herringbone structure. The 2 × 2 unit cell with larger area per molecule may be regarded as presenting the case of submonolayer structures for BZM and BT. The molecules of BZM still maintain almost vertical configuration while those of BT are much more tilted, but both monolayers do not form well-ordered structures on 2 × 2 unit cells, however.

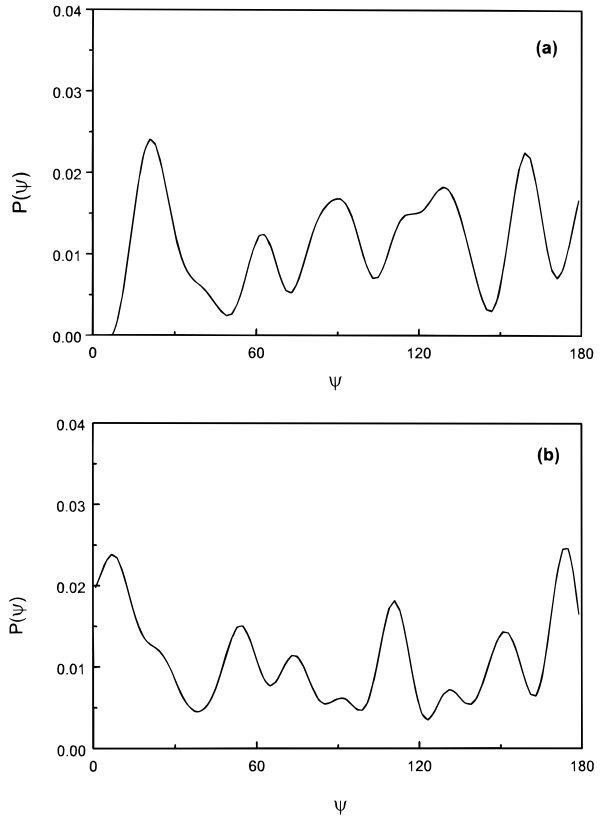

Figure 10. Distributions of the twist angle (ψ) for (a) BZM and (b) BT on 2 × 2 unit cells from the molecular dynamics simulations at 300 K.

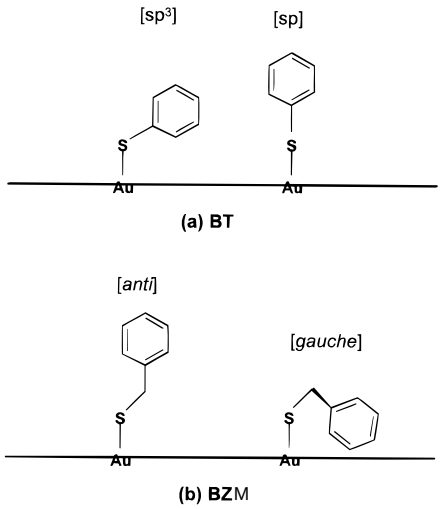

Figure 11. Possible structures of BT and BZM on the Au surface, drawn on a simple "single molecular basis".

Experimentally, the BZM was found to form a full-covered $\sqrt{3} \times \sqrt{3}R30°$ structure and the BT monolayer showed disorderd structure with the inverse bonding density of 38 Å^2/molecule.[11] The results of the present simulations discussed above provide plausible explanations for the experimental observation. The molecules of BZM, with the vertical configurations, can exhibit ordered

monolayers with herringbone structure when allowed to form full monolayers. During the process of self-assembly, both the methylene units and the benzene rings are expected to assume favorable orientations for the formation of the herringbone structure. The simulation results on $\sqrt{3} \times \sqrt{3}R30°$ unit cells suggest that BT can also form the herringbone-type structure. It can be argued that the herringbone structure is a thermodynamically stable structure for most of aromatic thiols. However, the molecules of BT have a strong tendency of assuming a rather "lying-flat" geometry with large tilt angles. In the stage of submonolayer formation, those molecules can be trapped in such a tilted structure and cannot proceed to form a close-packed full monolayer, which requires vertical configurations. Namely, the formation of close-packed herringbone structure is a kinetically unfavorable process for BT. This view is consistent with large area per molecule for BT SAMs.

A similar kind of kinetic trapping may be responsible for the finding that disordered structures are obtained for BZM on the $\sqrt{3} \times \sqrt{3}R30°$ unit cells when we have started the simulation with random orientations of methylene units. With the limited free space of a $\sqrt{3} \times \sqrt{3}R30°$ unit cell, it would be difficult to relieve the unfavorable orientations of the methylene units connected directly to the sulfur headgroup. In the actual formation of SAMs, it is more likely that the orientations of the methylene units are adjusted favorably in the submonolayer stage. Therefore, our simulations with all the methylene units made parallel for the initial configurations can be considered to provide relevant situations observed experimentally.

Considering that the structural difference between the two adsorbates is the absence or the presence of one methylene unit between the benzene ring and the sulfur headgroup, the methylene group itself should play a key role in the final two-dimensional arrangement of adsorbates on gold surfaces. In general, the first structural unit next to the sulfur headgroup will be crucial because it determines the freedom of overall orientation of the molecule. Having the flexible methylene unit at this position, the molecule can rotate rather freely to find a better orientation for the packing of the bulky groups attached, as in the case of the BZM monolayers. In fact, the flexibility of the methylene group is reflected in the barrier of the dihedral angle distortion of the $S-C_{methylene}-C_{ring}-C_{ring}$ bonds of BZM that is calculated to be at best about 2.4 kcal/mol (see Figure 3 and Table 1). There is no doubt that such a flexibility apparently assists in the formation of a close-packed structure by long alkanethiolates on gold. Without the flexible unit as in BT, it would be very difficult for the molecule to rotate around the chemisorbed sulfur bond, thereby the orientation of the benzene ring will be randomly distributed. It explains the difficulty of BT molecules to form vertical configurations once trapped in the tilted structure as discussed above. The importance of the methylene group can be gleaned from other examples. For instance, (4-mercaptophenyl)-phthalimide has been reported to assume disordered structures on Au(111);[19] similar disordered structure has been made even for a water-supported monolayer of $F(CF_2)_6(CH_2)_6OC_6H_4COOH$.[30] Nonetheless, it is also to be noted that highly ordered structures could be formed even for molecules that possess a benzene ring directly attached to a surface binding headgroup, particularly when the adsorbates are very rigid. Dhirani et al. observed the STM images of oligo(phenylethynyl)benzenethiolates on gold to be highly ordered, with the lattice vectors representing a $2\sqrt{3} \times \sqrt{3}R30°$ structure.[12]

As pointed out before, our calculations were very limited to the simulations only in two types of unit cells. The actual self-assembly mechanism is known to be very complex. In many cases, the self-assembly of organic thiols on Au(111) in a solution phase follows the Langmuir adsorption isotherm. In a gas-phase experiment, Poirier and Pylant observed that the formation of alkanethiolate monolayers on Au(111) followed a two-step process that began with condensation of low-density crystalline islands, characterized by surface-aligned molecular axes, from a lower density lattice-gas phase.[31] At saturation coverage, the monolayer underwent a phase transition to a denser phase by realignment of the molecular axes along the surface normal. The latter type transition should be strongly affected by the structural details of the molecules. It can be argued that such a transformation will be facilitated by the presence of the flexible part around the headgroup of the adsorbates, as likely in BZM. Regarding this matter, it is worthwhile to notice the MD simulations by Hautman and Klein[13,14] that alkanethiolate ($CH_3(CH_2)_{15}S^-$) should assemble on Au(111) with ordered and oriented chains uniformly tilted with respect to the surface normal, regardless of the constraint to be imposed on the orientation of S−C bond; to accommodate the stronger inter-alkyl chain interaction, the $S-C_{methylene}$ bond rotates readily.

As implied in the above discussion, the packing structures of condensed phase systems such as SAMs are determined mainly by the repulsive interactions reflecting the shapes of the molecules. The stability of such structures can be influenced by the collective attractions of the molecules. When the intermolecular interactions are strong enough, stable monolayer structures can be formed without strong attraction to the substrate. In the actual self-assembly of BT and BZM on gold, their azimuthal angle would be distributed randomly at the early stage. If the intermolecular (ring-to-ring) interaction is very favorable, not only BZM but also BT molecules will be packed to each other closely as the self-assembly proceeds, assuming a coherent tilt, twist, and azimuthal angle distribution. The observation that BT monolayers are not perfectly ordered at a full coverage limit suggests that the inter-ring interaction is not sufficient enough. The intermolecular interaction between BZM molecules should be hardly different from that between BT molecules. Then, the fact that BZM monolayers are well-ordered on Au(111) indicates that the inter-ring interaction can act favorably when a flexible group (like a methylene group) is connected directly to the benzene ring moiety.

Summary

For the first time we have demonstrated via MD simulations that BZM monolayers assume a well-ordered herringbone type packing on Au(111) while BT monolayers are disordered. Although the parameters used in this work were somewhat arbitrary, the final results were consistent with recent experimental observation. This work reveals the importance of a flexible group, bridging the aromatic ring and the sulfur headgroup, in producing close-packed structures of aromatic thiols on gold. We will continuously examine and modify the potential energy parameters, specifically related with the headgroups, by performing MD simulations on various BT and BZM derivatives. We plan to perform MD simulations allowing the diffusion of adsorbates on the Au(111) surface to examine the self-

(30) Gao, J.; Rice, S. A. *J. Chem. Phys.* **1993**, *99*, 7020.

(31) Poirier, G. E.; Pylant, E. D. *Science* **1996**, *272*, 1145.

assembly process itself. It will also be worthwhile to examine the effect of the bonding type (sp^3 and sp) of the sulfur headgroup on the packing structures of the present SAMs as has been done on related systems.[19]

Acknowledgment. This work was supported by the Korea Science and Engineering Foundation through the Center for Molecular Catalysis at Seoul National University (SNU) and by the Korea Research Foundation through the Research Institute for Basic Sciences at SNU.

LA9808667